Momentum and polarization dependence of single-magnon spectral weight for Cu L_3-edge resonant inelastic x-ray scattering from layered cuprates

L. Braicovich,[1] M. Moretti Sala,[1] L. J. P. Ament,[2] V. Bisogni,[3,4] M. Minola,[5] G. Balestrino,[6] D. Di Castro,[6] G. M. De Luca,[7] M. Salluzzo,[7] G. Ghiringhelli,[5] and J. van den Brink[4]

[1]*CNR-IOM and Dipartimento di Fisica, Politecnico di Milano, I-20133 Milano, Italy*

[2]*Institute-Lorentz for Theoretical Physics, Universiteit Leiden, 2300 RA Leiden, The Netherlands*

[3]*European Synchrotron Radiation Facility, Boîte Postale 220, F-38043 Grenoble, France*

[4]*Leibniz Institute for Solid State and Materials Research, IFW Dresden, 01171 Dresden, Germany*

[5]*CNR-SPIN and Dipartimento di Fisica, Politecnico di Milano, I-20133 Milano, Italy*

[6]*CNR-SPIN and Dip. di Ing. Meccanica, Università di Roma Tor Vergata, I-00133 Roma, Italy*

[7]*CNR-SPIN and Dip. Scienze Fisiche, Università di Napoli "Federico II," I-80126 Napoli, Italy*

(Received 29 March 2010; revised manuscript received 4 May 2010; published 27 May 2010)

Recently it was predicted theoretically and confirmed experimentally that in cuprates single-magnon dispersions can be mapped out with resonant inelastic x-ray scattering (RIXS) at the copper L_3 edge. To further establish RIXS as a viable technique we investigate the momentum and incident photon polarization dependence of the single-magnon spectral weight in a variety of layered undoped antiferromagnetic compounds. The agreement of experimental and theoretical results bolsters the assignment of RIXS spectral features to single magnons. This detailed analysis allows to disentangle single-magnon scattering from other spectral contributions. Moreover, it is a necessary premise for future research aimed at investigating processes that modulate spectral weights beyond the predictions of linear spin-wave theory.

DOI: 10.1103/PhysRevB.81.174533 PACS number(s): 74.72.Cj, 75.30.Ds, 75.25.−j, 78.70.Ck

I. INTRODUCTION

Strongly correlated electron systems are characterized not only by the energy and dispersion of their elementary excitations but also by the weight of these quasiparticle modes across the reciprocal space.[1] In doped cuprates, for instance, an understanding of the evolution of quasiparticle spectral weights is considered to be intimately related to the appearance of superconductivity at relatively high temperatures.[2] In this respect the midinfrared region, up to about ~0.5 eV, is of special interest in high-T_c superconducting cuprates as in this energy range both photon and magnetic spectroscopies reveal large spectral weight shifts upon doping.[3]

During the past decades the magnetic quasiparticles properties of cuprates have been studied exclusively with inelastic neutron scattering, providing a wealth of experimental information.[4] Recently, however, a different, photon-based approach called resonant inelastic x-ray scattering (RIXS) (Ref. 5) was introduced for the measurement of single-magnon dispersions.[6,7] This has opened prospects that can cross-fertilize with neutrons; in particular, the method can be used on tiny amounts of material (down to a few μm^3 in volume) while neutrons need comparatively massive samples (hundreds of mm^3 or more). Moreover, RIXS provides spectral information up to high-excitation energies where the use of neutrons is experimentally very demanding. On the other hand, the very low energy scale (below ~50 meV at present) remains the domain of neutrons because of the limited RIXS energy resolution, notwithstanding the spectacular progress in recent years.[7–10]

Measuring magnon energies and dispersions by RIXS has been the first step into a territory. To fortify the basis for RIXS in this field one needs to develop an understanding of both the position and the intensity of such spectral features. The former is directly related to the *position* of quasiparticle poles, the latter to their *strengths*. We have therefore set out to measure the dependence of the single-magnon RIXS spectral weight of undoped cuprates on momentum transfer, experimental geometry and incident photon polarization. This was done by closely comparing experimental results to theoretical expectations. The agreement found reinforces the assignment of some RIXS spectral features to single magnons and will allow us, in the future, to univocally disentangle single-magnon from bimagnon and higher order magnetic excitations.[11,12] In more general terms, this understanding is a necessary premise for future research on more complex processes, e.g., those involving strong quantum fluctuations of the Néel state[13,14] that can modify magnon quasi-particle spectral weights near the edge of the Brillouin zone (BZ).

We will mainly present results on La_2CuO_4 (LCO), which is one of the most extensively studied parent cuprates so that we can use it as a benchmark. When discussing form factor effects we also include experimental results on the infinite layer cuprate $(SrCa)CuO_2$ (SCCO) (which can be prepared in this form only as thin films on $SrTiO_3$) and of the strongly underdoped insulating $NdBa_2Cu_3O_{6+\delta}$ (NdBCO), which has the YBCO structure.

II. SINGLE-MAGNON DISPERSION IN RIXS

For a long time it was believed that selection rules prevent single-magnon (resonant) scattering in cuprates.[15,16] Recently, however, it was proven both theoretically and experimentally that single magnons can be observed with RIXS at the Cu L_3 edge.[6,7,17] It turns out that selection rules only forbid spin-flip scattering in cuprates when the spin is perpendicular to the basal plane—it is allowed however when there is a nonzero projection of the spin on the basal plane.[6]

In RIXS at the L_3 edge ($2p_{3/2} \rightarrow 3d$ resonant transition) a copper ion in a $3d^9$ ground state absorbs a photon with momentum $\mathbf{k}$ and polarization $\boldsymbol{\epsilon}$, causing the formation of a $2p^5 3d^{10}$ intermediate state, which subsequently decays into a final $3d^9$ state with a flipped spin, emitting a photon with momentum $\mathbf{k}'$ and polarization $\boldsymbol{\epsilon}'$. The momentum $\mathbf{q}=-(\mathbf{k}'-\mathbf{k})$ is transferred to a magnon and, because in the intermediate state the superexchange is blocked, in general also to higher-order spin excitations.[11,12]

In RIXS the final state excitations appear as photon energy losses that depend on the momentum $\mathbf{q}_\parallel$, i.e., the projection of $\mathbf{q}$ onto the *ab* plane of layered cuprates. The observed magnon dispersion in LCO, i.e., the evolution of magnon energy with the transferred momentum $\mathbf{q}_\parallel$ presented in Ref. 7, is well understood mainly thanks to the perfect agreement between RIXS results and inelastic neutron scattering data.[18] However, the evolution vs $\mathbf{q}_\parallel$ of the magnon peak intensities depends on the scattering geometry and on the incident photon polarization in a non trivial way. In particular there is no direct analogy with neutrons because the atomic form factors are unrelated for the two cases. Here, we will analyze the RIXS magnon intensities which reflect the magnon excitation probability and show how to maximize the sensitivity to magnons by taking advantage of the polarization of the incident light.

III. EXPERIMENTAL METHODS

The LCO, SCCO, and NdBCO samples were epitaxial films, approximately 100 nm thick, grown on $SrTiO_3$(001) substrate. LCO and SCCO were grown by pulsed laser deposition, NdBCO by diode high-pressure oxygen sputtering, of stoichiometric samples. More details on the samples can be found in Refs. 11, 19, and 20. The spectra were measured at the ADRESS beam line[21] of the Swiss Light Source with the high resolution SAXES spectrometer[8] with a combined linewidth of 140 meV at the Cu L_3 edge. Instruments and settings are similar to Ref. 7 and we collected the spectra with linear polarization of the incident light both perpendicular (σ-pol) and parallel (π-pol) to the scattering plane. The sample temperature was 15 K. $\mathbf{q}_\parallel$ was changed by rotating the sample as shown in Fig. 1(a), where we used two scattering angles (α=130° and 90°). For fixed α, by rotating the sample we can change δ (angle between $-\mathbf{q}$ and the surface normal that also coincides with the *c* crystalline axis) and $q_\parallel = q \sin\delta$; from the definition of δ and of the incidence angle θ given in the figure, it follows that $q_\parallel < 0$ toward grazing incidence ($\theta < \alpha/2$) and $q_\parallel > 0$ around normal incidence ($\theta > \alpha/2$). In this setup, scanning $q_\parallel$ necessarily implies changing θ thus leading to a modulation of the scattering cross section caused by the angular dependence of the atomic absorption and emission probabilities in a non spherical crystal field. In LCO we explored the two directions from Γ [point (0,0)] toward (± 1,0) and ($\pm 1, \pm 1$), all in the first BZ. For SCCO and NdBCO we measured only along the (± 1,0) direction. We notice that the maximum of $q_\parallel$ for 930 eV photons is 0.74 Å^{-1} for α=130° and 0.43 Å^{-1} for α =90°. This means that the magnetic BZ boundary can be reached only for α=130° in the ($\pm 1, \pm 1$) direction (the distance from Γ of the $(\frac{1}{2}, \frac{1}{2})$ point is ~0.60 Å^{-1}). For compactness, in the figures we use as unified momentum variable q_x, i.e., the component of $\mathbf{q}_\parallel$ along the (± 1,0) direction.

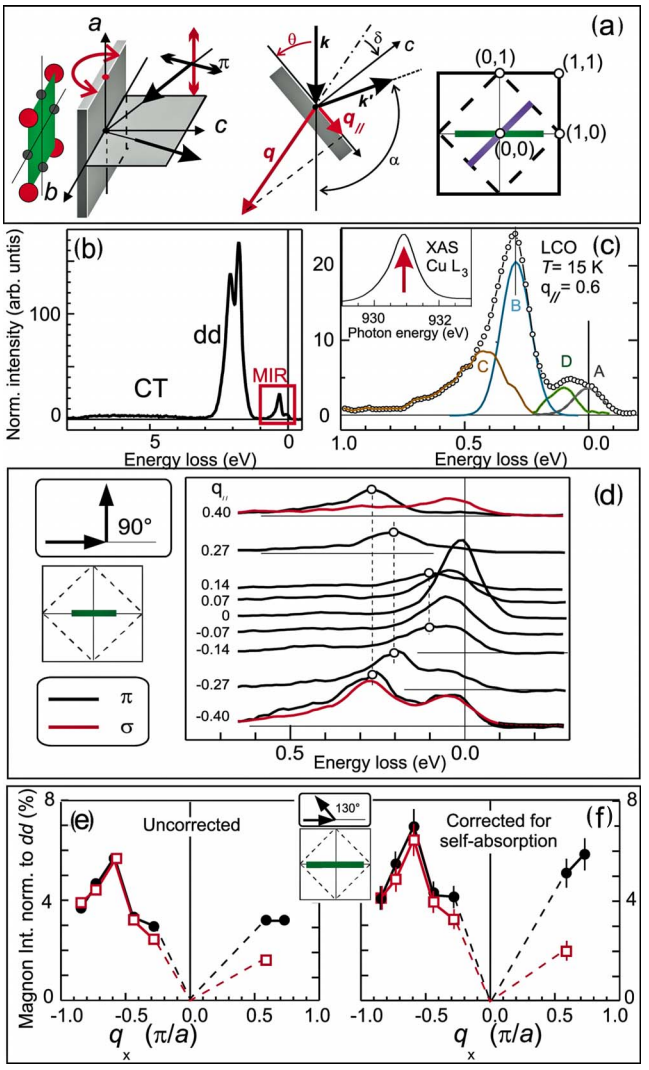

FIG. 1. (Color online) Panel (a): layout of the experiment and definition of angles α, δ, and θ. The $q_\parallel$ is varied by rotating the sample around the vertical axis; as $q_\parallel = q \sin\delta$, $q_\parallel > 0$ indicates near normal incidence geometry ($\theta > \alpha/2$). With the sample as in the figure one explores the green line in the BZ; the violet diagonal is explored after 45° rotation of the sample around its *c* axis. Panel (b): a RIXS spectrum of LCO. Charge transfer excitations are labeled with CT and the main peak is due to *dd* excitations; the MIR region (red box) is expanded in panel (c), where the magnon peak is labeled with B; peak A is the elastic intensity, feature C the multimagnon spectral distribution, peak D the partly unresolved phonon contribution, as explained in Ref. 7. Panel (d): example of dispersion of the magnetic excitations in LCO for α=90°, with intensities normalized to the *dd* area put to 100; note that the intensities are not symmetric with respect to $q_\parallel$=0. Panel (e) and (f): for α=130°, measured single magnon intensity normalized to the *dd* intensity as explained for panel (d). Full circles and hollow squares are for π an σ polarization respectively. Raw data are shown in panel (e), self-absorption corrected data in panel (f).

A typical spectrum of LCO in a wide energy range is shown in Fig. 1(b). The midinfrared (MIR) region, where the

magnetic excitations can be found,[7,10,11] is in the red box, which is expanded in Fig. 1(c) (reproduced[22] here from Ref. 7). The single magnon excitation (peak labeled B) is, in this example, more probable than multiple magnon excitations (peak C), so the peak position can be easily determined within 10–15 meV. As already stated its dispersion agrees well with the neutron results.[7,18]

IV. MEASURED MAGNON INTENSITIES

We extract the magnon intensities from the data by centering at the peak position a Gaussian with a width determined by the instrumental resolution.[23] It must be noted that in RIXS absolute intensities cannot be obtained from the experiment and the overall detection efficiency can change over time for technical reasons. It is thus necessary to use a spectral feature outside the MIR region as reference. We therefore normalize experimental and theoretical single magnon intensities to the area of the *dd* excitations, which largely dominate all the Cu L_3 RIXS spectra. This procedure might slightly underestimate ($\sim$5%) the single magnon intensity in the measured data, since superimposed to the *dd* peaks a weak contribution from the charge transfer excitations (not included in our theory) is always present. In the following by "intensity" we refer to the single magnon intensity normalized to the *dd* excitations, both for experimental and theoretical data.[6]

Two precautions are important in data handling. First, to be safe we do not attempt to determine intensities at small $q_\parallel$ where the superposition with other excitations such as phonons makes the spectral decomposition difficult as far as the intensities are concerned. Second, one has to correct for self-absorption. In terms of deformation of the q dependence this is relevant only at grazing emission, i.e., at large positive $q_\parallel$ where the scattered photons undergo a long path inside the strongly reabsorbing material. In general the linear polarization is not conserved in the scattering process, so the correction is delicate and has to rely upon the knowledge of the outgoing photon polarization (also calculated within the atomic model). This correction is demonstrated in Figs. 1(e) and 1(f), showing raw and absorption-corrected data, respectively. It is important to note that the large difference between π polarization (in black) and σ polarization (in red) at large positive $q_\parallel$ is already clearly present in the raw data.

V. RESULTS AND DISCUSSION

It is illuminating to start with a close inspection of the 90° scattering data [Fig. 1(d)]. It is immediately clear that while the dispersion is symmetric in $q_\parallel \rightarrow -q_\parallel$ as it must be, the intensities are not, and this asymmetry is much stronger for σ than π polarization. In fact the intensity is extremely small for σ polarization at $q_\parallel > 0$.

Figure 2 summarizes the full data set of intensity measurements. We compare the data directly to the theoretical results indicated by solid lines. Panels (a), (b), and (c) have the same scale so that comparison is straightforward. With the exception of the shaded area in panel (b) (see below) the theory reproduces the experimental trends very well, including the asymmetry for $q_\parallel \rightarrow -q_\parallel$. Theory captures correctly the intensity variation with both transferred momentum $q_\parallel$ and scattering angle, in particular for σ polarization, with $q_\parallel > 0$, where the intensity drops for α going from 130° to 90°. It should be noted that the theoretical results were rescaled by 0.8 to get the best fit to the data. Considering the error bars and the fact that the experimental normalized intensities are underestimated by at most 5%, we conclude that the agreement is also quantitative within the experimental uncertainties.

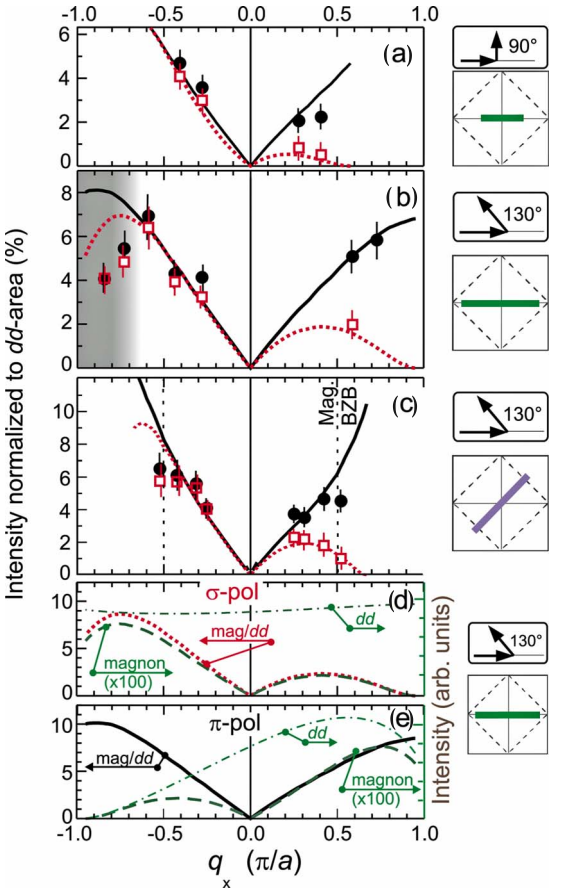

FIG. 2. (Color online) Panels (a)–(c): comparison of the normalized intensities in LCO with the theory in the conditions shown by the icons at the right. Panel (d) and (e): theoretical normalized intensity (red dotted and black solid, left scale) obtained by dividing the non-normalized intensity multiplied by 100 (thick dashed green, right scale) by the total *dd* intensity (thin dash-dot green, right scale) for σ and π polarizations, respectively. We notice that, at $q_\parallel < 0$, this normalization has a strong effect for π but very little for σ.

Theoretical and experimental results differ significantly only in the shaded region of Fig. 2(b), a case very little affected by self-absorption. We notice that for large values of $|q_\parallel|$, i.e., close to the BZ boundary, one could expect quantum corrections to the magnon quasiparticle spectral weight, as already observed with neutrons in copper deuteroformate tetradeurate (CFTD).[14] There, a transfer of spectral intensity is caused by quantum effects that are beyond the linear spin-wave approximation that we have employed here: it will be interesting to explore this quasiparticle renormalization in detail in future RIXS investigations.

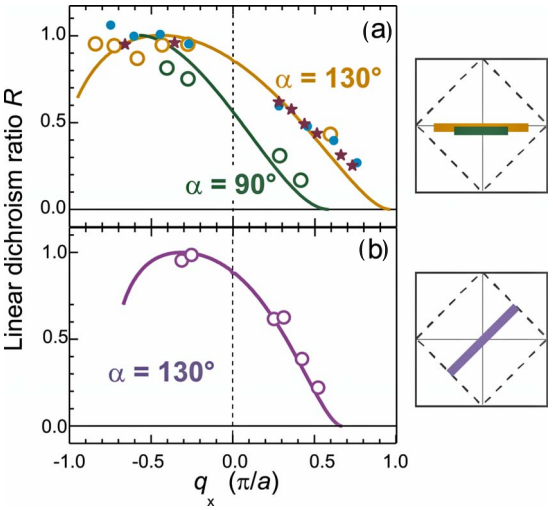

FIG. 3. (Color online) Comparison between experimental (symbols) and theoretical (lines) values of the linear dichroic ratio R (see text for the definition). The open points refer to LCO, the blue dots to SCCO, and the purple stars to NdBCO.

The comparison between theory and experiment also allows the atomic form factor $F(\boldsymbol{\epsilon},\boldsymbol{\epsilon}',\omega)$ to be extracted from the experimental data. The procedure for doing so relies upon the fact that the theoretical cross section and thus the scattering intensity can be written as[6] $I=F(\boldsymbol{\epsilon},\boldsymbol{\epsilon}',\omega)G(\mathbf{q})$, where the function $G(\mathbf{q})$ depends on the transferred momentum $\mathbf{q}$ only, while the polarization dependence is completely accounted for by the atomic form factor F, which determines the local spin flip probability for an atomic $3d^9$ ground state with a hole in the x^2-y^2 orbital. All the RIXS specific properties are in F, whereas $G(\mathbf{q})$ is technique independent and would be the same for inelastic neutron scattering. The $q_\parallel$ dependence of I is shown in Figs. 2(d) and 2(e) for σ and π polarization respectively (scale to the right, green dashed curves). In the same panels the total intensity of the dd excitations are also shown: although dd excitations are usually nondispersing, their intensity depends on the scattering geometry and on the photon polarization. The ratio of the two previous functions gives the function $\underline{I}$, referred to the left scale and shown in the same panels as red dotted and black solid lines for σ and π polarization respectively.

It is useful at this point to introduce the linear dichroic ratio $R=I_\sigma/I_\pi=\underline{F}_\sigma/\underline{F}_\pi$, where I is the normalized intensity and $\underline{F}$ is the atomic spin-flip form factor normalized to the total dd spectral weight. Thus R depends on the atomic form factors only and does *not* depend on $G(\mathbf{q})$. One can therefore test the calculated atomic form factors by directly comparing the theoretical linear dichroic ratio R to the experimental one. We do so in Fig. 3, where one should note that these curves are extracted directly from experimental and theoretical data, respectively, without any free parameters. The agreement is excellent for both directions in $\mathbf{q}$ space and both scattering angles. To further test the linear dichroic ratio we also measured R in SCCO and NdBCO, two undoped cuprates with different crystal structure than LCO. Despite the differences in the crystal structure, both materials, similar to LCO, are undoped and insulating with Cu^{2+} ions in a (nominal) $3d^9$ configuration, corresponding to a ground state with a single x^2-y^2 hole. As shown in Fig. 3(a) the R values for these two samples follow the theoretical curve as well as for LCO.

The results on R are a very reliable test of our picture because the experimental values of the linear dichroic ratio are less affected by self-absorption and instrumental effects than the intensities themselves. We thus conclude that the RIXS form factor is captured correctly by an atomic calculation.[6] Since we have shown above that the product $F\times G$ is also in agreement with the measurements we conclude that the theoretical $G(\mathbf{q})$ is correctly reproduced in the experimental data. It is particularly important to note that both factors F and G are independent of the specific magnetic and structural properties of the material, and are thus applicable potentially to all layered cuprates. As it appears clearly from the theoretical plots of Fig. 2 the normalized intensity $\underline{I}=\underline{F}\times G$ is not symmetric with respect to $q_\parallel=0$ and goes to zero at $q_\parallel=0$. The latter fact is totally due to G, which is zero at $q_\parallel=0$ and is symmetric in $+q_\parallel\rightarrow-q_\parallel$. On the other hand the atomic form factor F has an angular dependence dictated exclusively by the tetragonal crystal field imposing a x^2-y^2 symmetry in the ground state, and by the angular momentum conservation rules (depending on the photon polarization) in the radiative transitions between $2p$ and $3d$ orbitals. So F has no physical relation to $q_\parallel$, and the same holds for the normalized factor $\underline{F}$. Thus the lack of symmetry of $\underline{I}$ is inherently due to the fact that RIXS is a resonant process, going through an excitonic intermediate state and whose F function is remarkably well described by a totally localized model. Before concluding we notice the different behavior of $\underline{I}$ along $(\pm1,0)$ and along $(\pm1,\pm1)$ directions due to G. In the former case G is known to have a local maximum in (1,0), in the latter it diverges at (1,1). This difference appears immediately for π polarization when comparing panels (b) and (c) of Fig. 2.

VI. CONCLUSIONS

We have measured and calculated the momentum and photon polarization dependence of the single-magnon RIXS spectral weight in a number of undoped cuprates and find excellent agreement. The measured structure factor governing local spin-flip probabilities at the Cu L_3 edge fully agrees with the one given by an atomic calculation. The theoretical cross section validated here will be the basis for the interpretation of RIXS spectral weights in more complex materials, for instance, the doped superconducting cuprates, where the weights of quasiparticles and their redistribution upon doping are heavily debated and the charge and magnetic responses of the system are intrinsically intertwined.

ACKNOWLEDGMENTS

This work was performed at the ADRESS beam line of the SLS (PSI) using the SAXES spectrometer developed jointly by Politecnico di Milano, SLS, and EPFL. We wish to

thank M. Grioni, M. Haverkort, and H. M. Rønnow for illuminating discussions. One of us (L.B.) is indebted to LuBac for stimulating discussions and support. This research benefited from the RIXS collaboration supported by the Computational Materials Science Network (CMSN) program of the Division of Materials Science and Engineering, U.S. Department of Energy (Grant No. DE-FG02-08ER46540) and is supported by the Dutch Science Foundation FOM.

[1] H. Eskes, M. B. J. Meinders, and G. A. Sawatzky, Phys. Rev. Lett. **67**, 1035 (1991).
[2] M. R. Norman, H. Ding, M. Randeria, J. C. Campuzano, T. Yokoya, T. Takeuchi, T. Takahashi, T. Mochiku, K. Kadowaki, P. Guptasarma, and D. G. Hinks, Nature (London) **392**, 157 (1998).
[3] B. Keimer, A. Aharony, A. Auerbach, R. J. Birgeneau, A. Cassanho, Y. Endoh, R. W. Erwin, M. A. Kastner, and G. Shirane, Phys. Rev. B **45**, 7430 (1992); B. Keimer, N. Belk, R. J. Birgeneau, A. Cassanho, C. Y. Chen, M. Greven, M. A. Kastner, A. Aharony, Y. Endoh, R. W. Erwin, and G. Shirane, *ibid.* **46**, 14034 (1992).
[4] J. M. Tranquada, in *Handbook of High-Temperature Superconductivity*, edited by J. R. Schrieffer and J. S. Brooks (Springer, New York, 2007), pp. 257–298.
[5] A. Kotani and S. Shin, Rev. Mod. Phys. **73**, 203 (2001).
[6] L. J. P. Ament, G. Ghiringhelli, M. Moretti Sala, L. Braicovich, and J. van den Brink, Phys. Rev. Lett. **103**, 117003 (2009).
[7] L. Braicovich, J. van den Brink, V. Bisogni, M. Moretti Sala, L. J. P. Ament, N. B. Brookes, G. M. De Luca, M. Salluzzo, T. Schmitt, V. N. Strocov, and G. Ghiringhelli, Phys. Rev. Lett. **104**, 077002 (2010).
[8] G. Ghiringhelli, A. Piazzalunga, C. Dallera, G. Trezzi, L. Braicovich, T. Schmitt, V. N. Strocov, R. Betemps, L. Patthey, X. Wang, and M. Grioni, Rev. Sci. Instrum. **77**, 113108 (2006).
[9] G. Ghiringhelli, A. Piazzalunga, C. Dallera, T. Schmitt, V. N. Strocov, J. Schlappa, L. Patthey, X. Wang, H. Berger, and M. Grioni, Phys. Rev. Lett. **102**, 027401 (2009).
[10] J. Schlappa, T. Schmitt, F. Vernay, V. N. Strocov, V. Ilakovac, B. Thielemann, H. M. Rønnow, S. Vanishri, A. Piazzalunga, X. Wang, L. Braicovich, G. Ghiringhelli, C. Marin, J. Mesot, B. Delley, and L. Patthey, Phys. Rev. Lett. **103**, 047401 (2009).
[11] L. Braicovich, L. J. P. Ament, V. Bisogni, F. Forte, C. Aruta, G. Balestrino, N. B. Brookes, G. M. De Luca, P. G. Medaglia, F. Miletto Granozio, M. Radovic, M. Salluzzo, J. van den Brink, and G. Ghiringhelli, Phys. Rev. Lett. **102**, 167401 (2009).
[12] J. van den Brink, EPL **80**, 47003 (2007); F. Forte, L. J. P. Ament, and J. van den Brink, Phys. Rev. B **77**, 134428 (2008).
[13] M. Grüninger, D. van der Marel, A. Damascelli, A. Erb, T. Nunner, and T. Kopp, Phys. Rev. B **62**, 12422 (2000).
[14] N. B. Christensen, H. M. Rønnow, D. F. McMorrow, A. Harrison, T. G. Perring, M. Enderle, R. Coldea, L. P. Regnault, and G. Aeppli, Proc. Natl. Acad. Sci. U.S.A. **104**, 15264 (2007).
[15] F. M. F. de Groot, P. Kuiper, and G. A. Sawatzky, Phys. Rev. B **57**, 14584 (1998).
[16] M. van Veenendaal, Phys. Rev. Lett. **96**, 117404 (2006).
[17] M. W. Haverkort, arXiv:0911.0706 (unpublished).
[18] R. Coldea, S. M. Hayden, G. Aeppli, T. G. Perring, C. D. Frost, T. E. Mason, S. W. Cheong, and Z. Fisk, Phys. Rev. Lett. **86**, 5377 (2001).
[19] G. Balestrino, R. Desfeux, S. Martellucci, A. Paoletti, G. Petrocelli, A. Tebano, B. Mercey, and M. Hervieu, J. Mater. Chem. **5**, 1879 (1995).
[20] M. Salluzzo, G. M. de Luca, D. Marre, M. Putti, M. Tropeano, U. Scotti di Uccio, and R. Vaglio, Phys. Rev. B **72**, 134521 (2005). In order to reduce the oxygen content and obtain undoped NdBCO films, the sample has been annealed in an Argon atmosphere (10 mbar) for 24 h.
[21] V. N. Strocov, T. Schmitt, U. Flechsig, T. Schmidt, A. Imhof, Q. Chen, J. Raabe, R. Betemps, D. Zimoch, J. Krempasky, A. Piazzalunga, X. Wang, M. Grioni, and L. Patthey, arXiv:0911.2598 (unpublished).
[22] Note that the units of $q_{\|}$ have changed so that the BZ boundary is at $q_{\|}=1$ in the present article instead of π in Ref. 7.
[23] With 140 meV full width at half maximum resolution the final state magnon lifetime has marginal effects, if any.